

Supporting Information

Multicompartment Photonic Microcylinders toward Structural Color Inks

Gun Ho Lee[†], Tae Yoon Jeon[†], Jong Bin Kim[†], Byungjin Lee[‡], Chang-Soo Lee[‡], Su Yeon Lee^{*,§} and Shin-Hyun Kim^{*,†}

[†]Department of Chemical and Biomolecular Engineering (BK21+ Program), Korea Advanced Institute of Science and Technology (KAIST), Daejeon 34141, Republic of Korea

[‡]Department of Chemical Engineering and Applied Chemistry, Chungnam National University, Daejeon 34134, Republic of Korea

[§]Division of Advanced Materials, Korea Research Institute of Chemical Technology (KRICT), Daejeon 34114, Republic of Korea

* To whom correspondence should be addressed. E-mail: kim.sh@kaist.ac.kr and sylee@kRICT.re.kr

Supplementary Figures

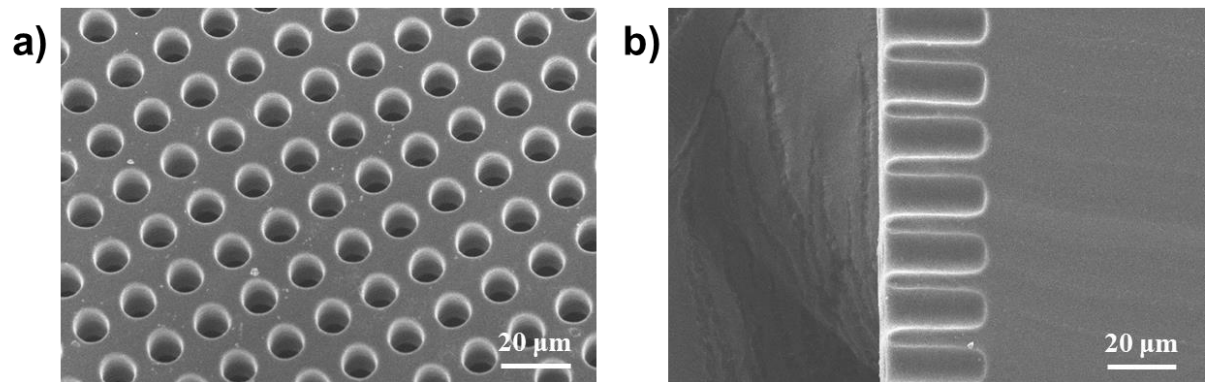


Figure S1. SEM images of a PDMS mold containing the array of cylindrical holes with a diameter of 10 μm and a depth of 23 μm: (a) Top view and (b) Cross-section view.

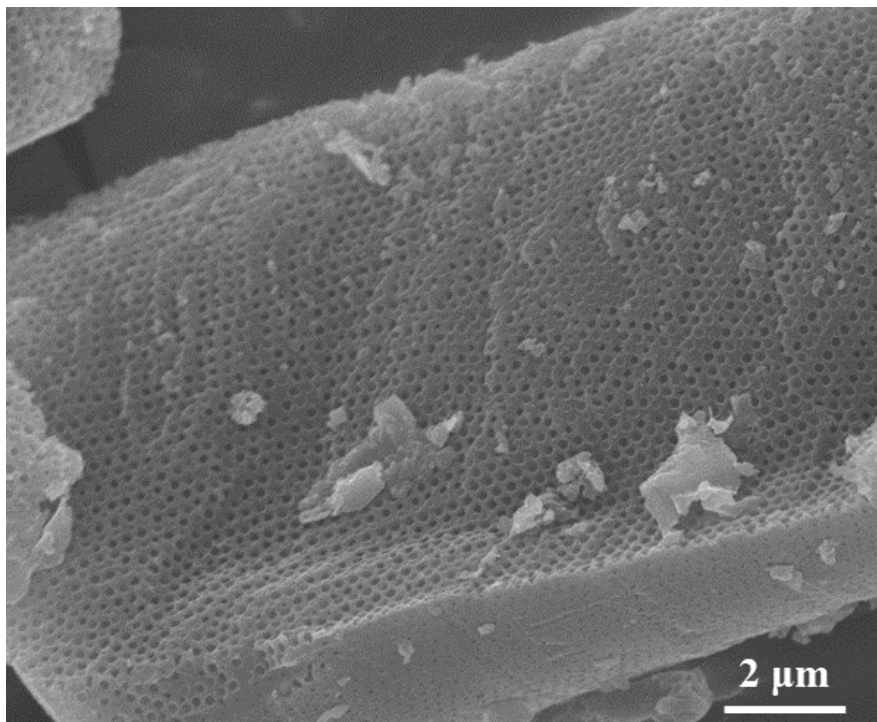


Figure S2. SEM image showing internal structure on a cross-section along the cylindrical axis of photonic microcylinder.

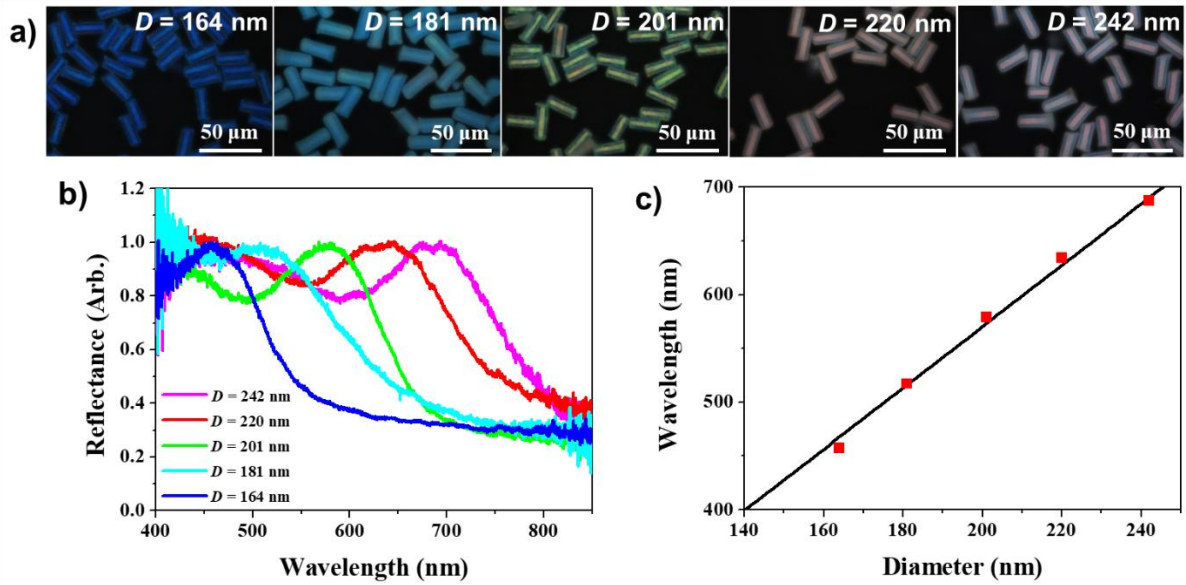


Figure S3. (a) A set of OM images of porous microcylinders, where silica particles with five different diameters of 164 nm, 181 nm, 201 nm, 220 nm, and 242 nm are used from the leftmost panel, while maintaining the volume fraction of 0.33. (b) Reflectance spectra of the porous microcylinders in (a). (c) Reflectance peak position of porous microcylinders as a function of the diameter of silica particles. The black line indicates Bragg's equation for stacked (111) planes of fcc structures, eq 1.

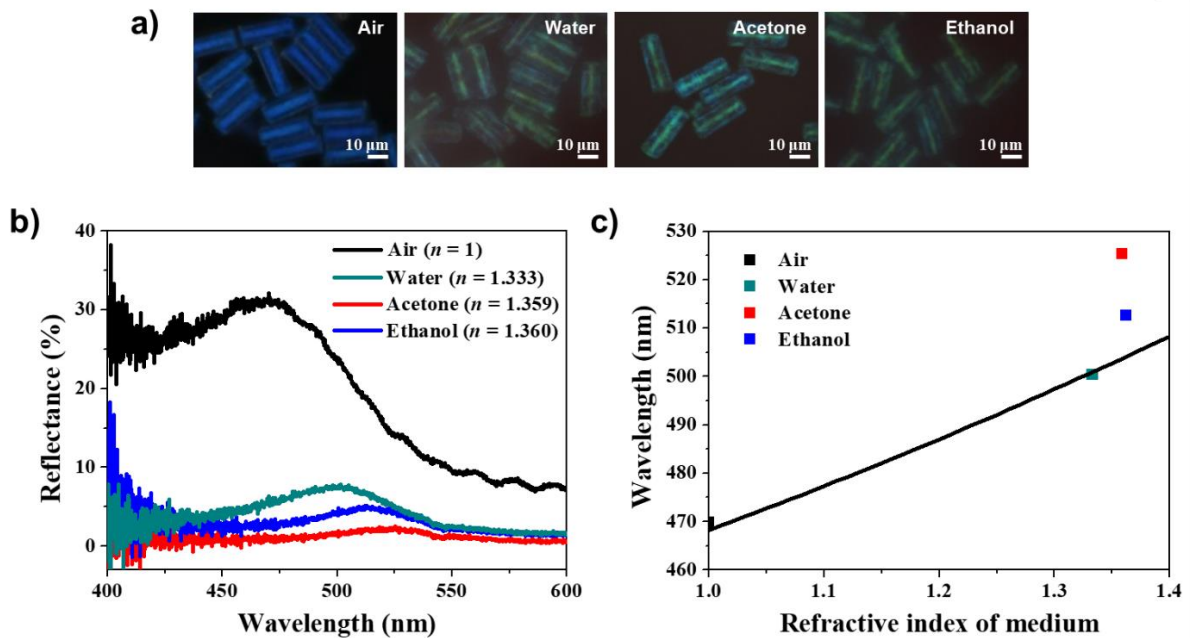


Figure S4. (a, b) A set of OM images and reflectance spectra of porous microcylinders dispersed in four different media: air, water, acetone, an ethanol. (c) Reflectance peak position for four dispersion media. A solid line indicates Bragg's diffraction for microcylinders whose pores are occupied with the media without lattice expansion.

The diffraction wavelength for porous microcylinders can be estimated by Bragg's law for stacked (111) planes of nonclose-packed fcc:

$$\lambda = 2d_{111}n_{eff} = \left(\frac{\pi}{3\sqrt{2}\phi}\right)^{1/3} \left(\frac{8}{3}\right)^{1/2} D \left(n_{cavity}^2\phi + n_{matrix}^2(1-\phi)\right)^{1/2}. \quad [1]$$

When the porous microcylinders are suspended in a solvent, the pETPTA matrix is swollen, which alters the values of ϕ and n_{matrix} . We define a swelling ratio, α as:

$$\alpha = \frac{1-\phi_f}{1-\phi_i} \left(\frac{a_f}{a_i}\right)^3, \quad [2]$$

where a_i and a_f are lattice constants of fcc before and after swelling and ϕ_i and ϕ_f are volume fractions of cavities before and after swelling, respectively. With an the refractive indices of swollen matrix and cavities can be respectively estimated as

$$n_{matrix}^2 = n_{pETPTA}^2 \frac{1}{\alpha} + n_{solvent}^2 \left(1 - \frac{1}{\alpha}\right) \quad \text{and} \quad n_{cavity} = n_{solvent}. \quad [4]$$

The swelling ratio, α , can be estimated from the wavelength of reflectance peak using the eq. 1 combined with eq. 3 and eq. 4.

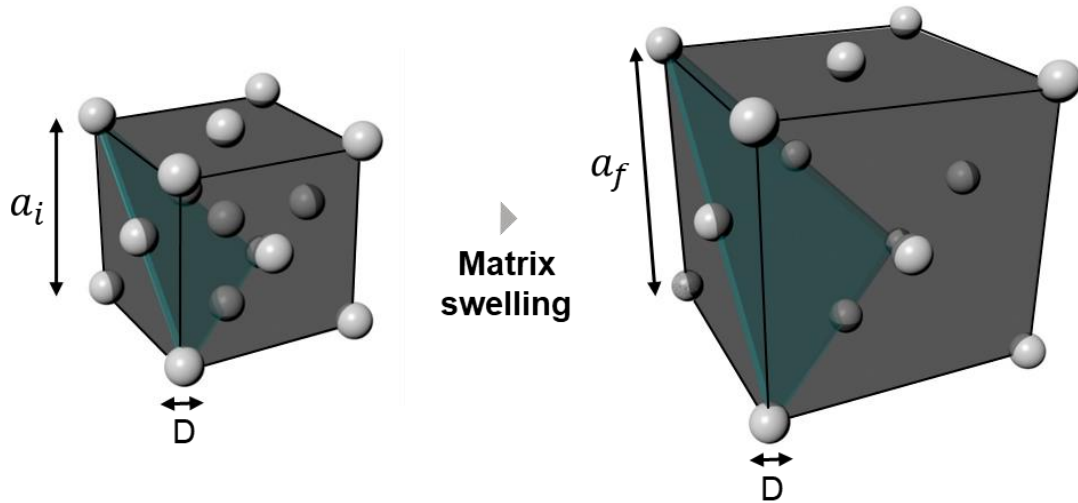


Figure S5. Schematic illustration showing the matrix swelling of an fcc unit cell.

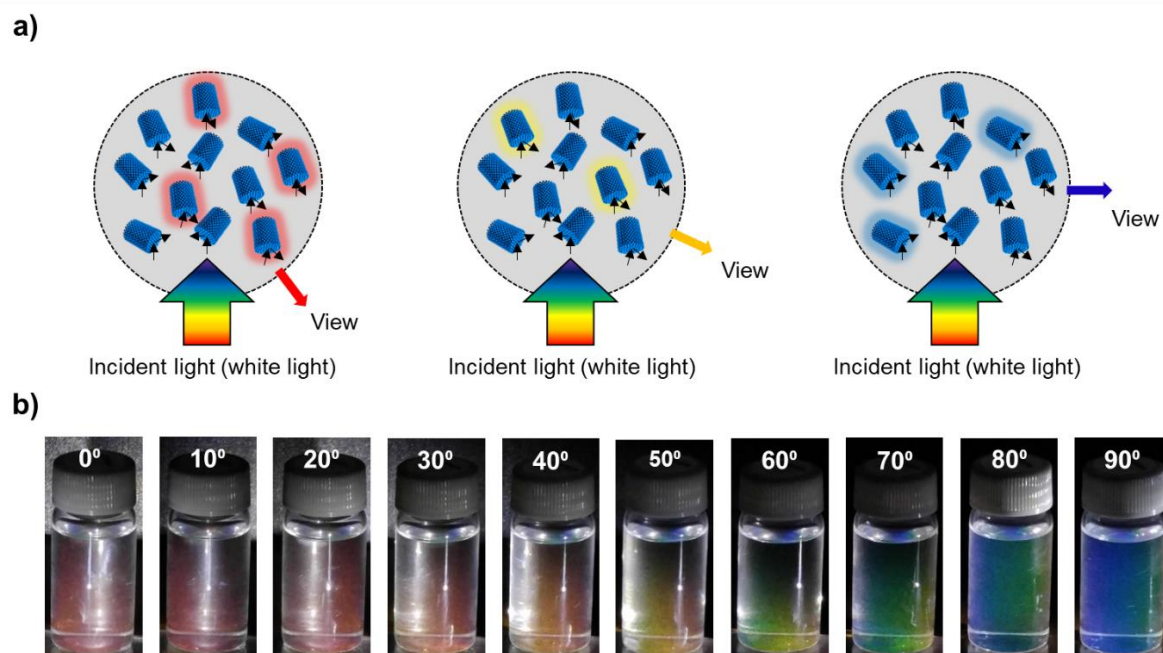


Figure S6. (a) Schematic illustrations showing an angle-dependent reflection of incident light by photonic microcylinders with a random orientation. Only the microcylinders that satisfy the reflection condition contribute to the structural color for a given angle between the incident light and observation. (b) A series of photographs showing the angle-dependent color of a microcylinder suspension, where the angle is denoted in each panel.

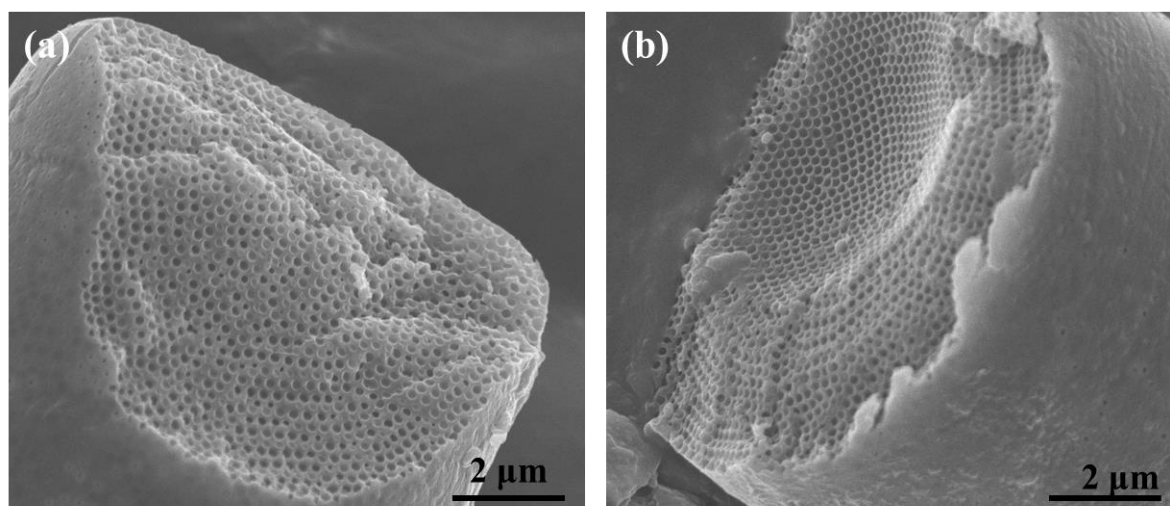


Figure S7. (a, b) SEM images showing cross-sections of photonic microcylinders prepared from ethanol-free silica-ETPTA dispersion (a) and 70% ethanol (b).

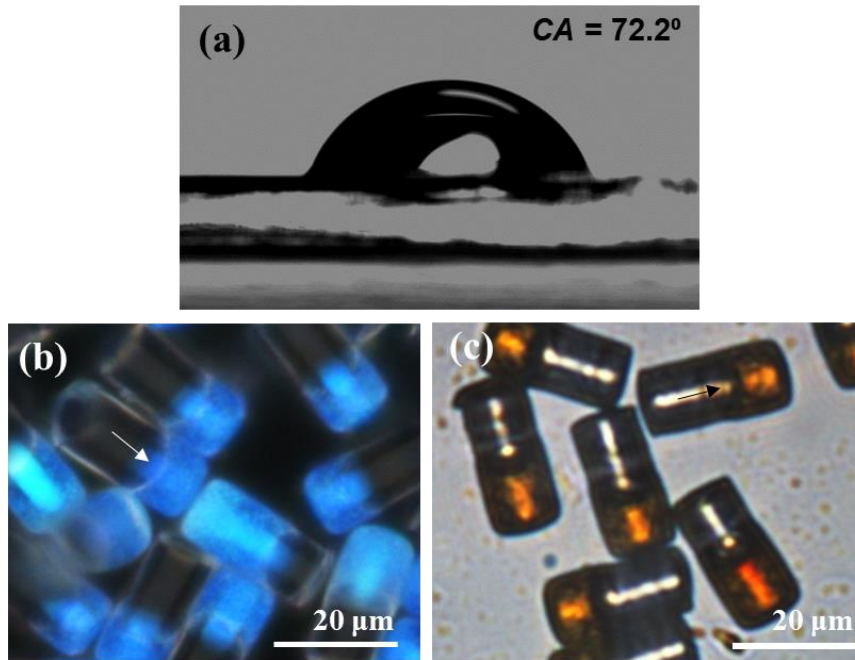


Figure S8. (a) Image showing a contact angle (CA) of ETPTA drop on PDMS film in air. CA is measured as 72.2° . The same CA is expected in the ETPTA dispersion that partially occupies cylindrical holes in the PDMS mold. (b, c) OM images of microcylinders composed of photonic and transparent compartments taken in reflection mode (b) and transmission mode (c). The boundary between the transparent and photonic compartment is concave upward as indicated by arrows. The blue compartment in reflection mode turns to orange in transmission mode.

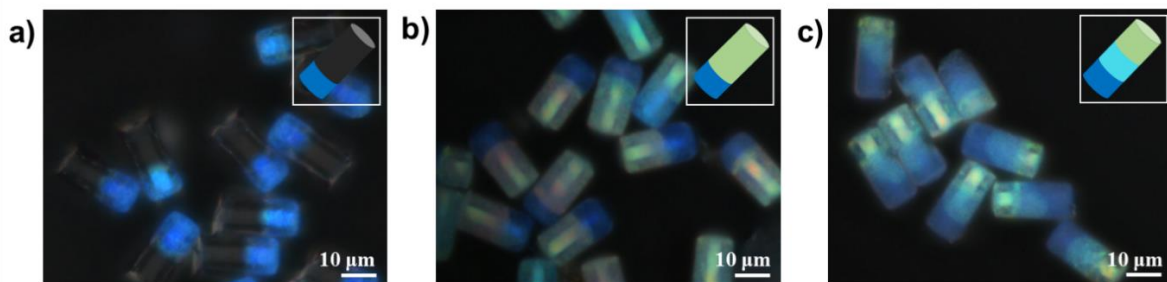


Figure S9. (a-c) OM images of photonic microcylinders composed of multiple compartments: (a) microcylinders with blue-colored and transparent compartments, (b) microcylinders with blue- and green-colored compartments, and (c) microcylinders with blue-, cyan-, and green-colored compartments. Insets are cartoons for the corresponding photonic microcylinders.

Description for Supplementary Movies

Movie S1: A suspension of photonic microcylinders which shows a blue shift of reflection color along with the angle between the incident light and the observation.

Movie S2: Collective motion of microcylinders under external magnetic field. The microcylinders align their orientation with the field direction.

Movie S3: Real-time tuning of color brightness by controlling the orientation of microcylinders with the external magnetic field.